



Indian Academy of Sciences, Bengaluru
Indian National Science Academy, New Delhi
The National Academy of Sciences, India, Prayagraj



SUMMER RESEARCH FELLOWSHIP, 2023

PROJECT REPORT ON

Detection of variable stars in the star cluster NGC 6709

Submitted by

Raghav Sandip Wani

PHYS2417

Indian Institute of Science Education and Research, Pune

Under the guidance of

Dr. Yogesh C. Joshi

Aryabhata Research Institute of Observational Sciences (ARIES), Nainital

Table of contents:

1. Introduction	4
2. Variability	4
2.1 Intrinsic Variable Stars	4
2.2 Extrinsic Variable Stars	5
3. Star Cluster	6
3.1 Globular clusters	6
3.2 Open clusters	6
3.2.1 NGC 6709	7
4. Data Acquisition and processing	8
4.1 Cleaning	9
4.2 Aperture Photometry	10
4.3 Calibration	12
4.4 Light Curves Analysis	14
4.5 Period and Phase estimation	15
5. Summary and conclusion	17
6. References	18

Table of contents for Figures

2.1: Flow Chart of types of variable stars	5
3.1: Star cluster comparison	7
3.2: Position of NGC 6709	8
4.1: Uncleaned and cleaned images of NGC 6709	10
4.2: Apertures	11
4.3: Growth curve	12
4.4: Calibration curve	13
4.5: Light curves	14-15
4.6: Phase - Magnitude curves	16-17

1. Introduction:

This is the final report for Indian Academy of Sciences Summer Research Fellowship Program 2023. The report covers details of detection of variable stars in the open star cluster NGC 6709. The data used in this report was collected from 130-cm Devasthal Fast Optical Telescope (DFOT) in R band over a time period of about a year. Here we have used a python script for performing tasks of image cleaning, aperture photometry, calibration and plotting light curves of detected variable stars of the cluster.

2. Variability:

Variability is a property of most stars, and as such it has a great deal to contribute to our understanding of them. It provides us with additional parameters (time scales, amplitudes, etc.) which are not available for non-variable stars. These parameters can be used to deduce physical parameters of the stars like mass, radius, luminosity, period of rotation, etc. or to compare with theoretical models. We can choose a ‘model’ of a given star by requiring that it reproduce the observed variability as well as the other observed characteristics of the star. From the model, we can then learn about the internal composition, structure, and physical processes in the star.

Because the variations provide important and often-unique information about the nature and evolution of the stars. This information can be used to deduce even more fundamental knowledge about our universe in general. The variations may be due to the rotation of a spotted star, or to an eclipse of a star by a companion star, or even by an unseen planet. The variations may be due to the vibrations of a star, eruptions on a star (flares), accretion disc (dwarf novae), explosions on a star (novae), or to the total disruption of a star like in a supernova. Variable stars exhibit different types of variability, and their classifications are based on various factors such as the nature of the variability, the cause of the variations, and their characteristics in terms of light curves and spectral properties. They can be classified into two main categories: intrinsic variable stars and extrinsic variable stars.

2.1 Intrinsic Variable Stars:

Intrinsic variable stars are those that undergo brightness variations due to physical processes occurring within the star itself. These variations are typically attributed to changes in the stellar structure, pulsations, eruptions, or other internal mechanisms. Intrinsic variable stars can be further classified into various subtypes:

- *Pulsating variables*: These stars undergo regular expansions and contractions, resulting in periodic changes in brightness. Examples include Cepheid variables, RR Lyrae stars, and Delta Scuti stars.
- *Eruptive variables*: These stars experience sudden and dramatic increases in brightness due to violent outbursts or explosions. Examples include novae and supernovae.

- *Cataclysmic variables*: These stars undergo large and rapid changes in brightness due to interactions with a close companion star, often in a binary system. Examples include dwarf novae and recurrent novae.

2.2 Extrinsic Variable Stars:

Extrinsic Variable Stars are stars where the variability is caused by the external properties like rotation or eclipses. There are two main subgroups.

- *Eclipsing Binaries*: These are double star systems where, as observed from Earth, one star periodically eclipses the other as they orbit around a common center of mass. The eclipses result in periodic decreases in brightness. Eclipsing binaries are an important class of extrinsic variable stars and provide valuable information about the system's parameters, such as orbital periods, sizes, and masses of the stars.
- *Rotating Variables*: These are stars whose variability is caused by phenomena related to their rotation. Examples include stars with significant surface features like sunspots or stars with rapid rotation, which can lead to oblate or ellipsoidal shapes. The changing appearance due to rotation results in variations in brightness. Rotating variables are another subset of extrinsic variable stars, where the observed variability arises from the star's rotation rather than internal processes.

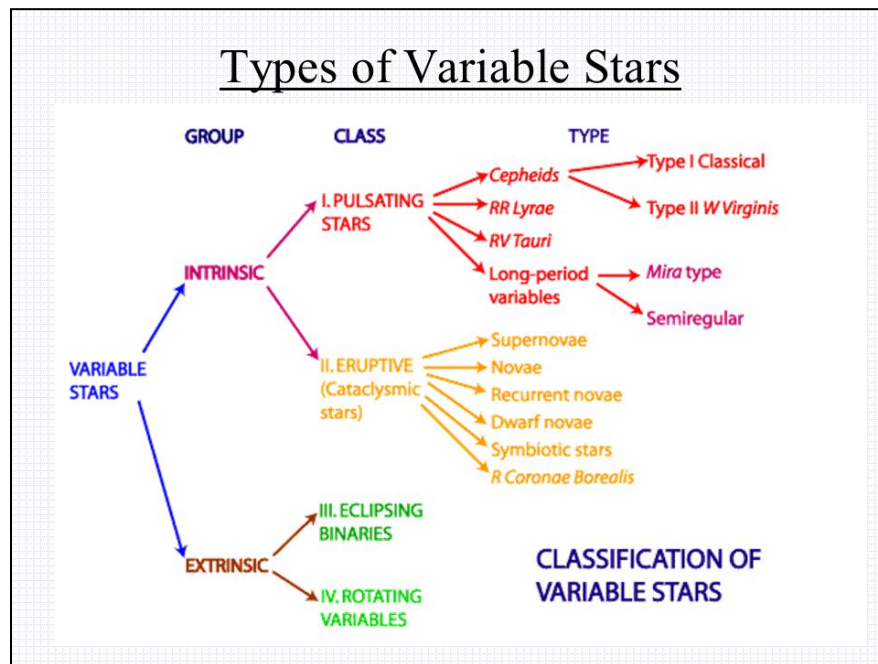


Figure 2.1: Flow Chart of types of variable stars.

The figure 2.1 summarizes the types of variable stars. Understanding the characteristics and behavior of variable stars, whether intrinsic or extrinsic, provides valuable insights into stellar physics, stellar evolution, and the dynamics of binary star systems. These observations help astronomers study fundamental properties of stars, such as distance determinations,

luminosities, and chemical compositions, ultimately contributing to our broader understanding of the universe.

3. Star Cluster:

Star clusters are invaluable objects of study in the field of astrophysics, providing significant insights into stellar evolution, star formation processes, and the dynamics of galaxies. They exist in two main forms: globular clusters and open clusters. Both globular and open clusters serve as vital tools for astronomers to determine distances within the cosmos. By employing various distance determination techniques, such as main-sequence fitting, stellar evolution models, and astrometric measurements, researchers can establish accurate distances to star clusters. These distance measurements, in turn, help constrain the cosmic distance ladder and provide fundamental inputs for calibrating other distance indicators in the universe.

3.1 Globular clusters:

Globular clusters are densely packed spherical or elliptical clusters containing hundreds of thousands to millions of stars. They are primarily found in the outer regions of galaxies, orbiting around the galactic core. These clusters typically exhibit a high degree of stellar stability and longevity, lasting for billions of years. The stars within globular clusters are predominantly old, often billions of years in age, and possess similar compositions, making them ideal for investigating stellar populations of different ages and chemical abundances. Their unique properties provide researchers with essential information about the early stages of galaxy formation, as well as the structure and dynamics of galactic systems. Notable examples of globular clusters include Messier 13 (M13) in the constellation Hercules and Omega Centauri (NGC 5139) in the constellation Centaurus.

3.2 Open clusters:

In contrast, open clusters, also known as galactic clusters or stellar associations, are less densely populated and contain a few dozen to a few thousand stars. They are predominantly located within the disk of galaxies, such as our Milky Way. Open clusters consist of relatively young stars, typically ranging from a few million to a few hundred million years old. Due to their youthful nature, open clusters are excellent laboratories for studying stellar evolution, star formation processes, and the effects of stellar interactions. Over time, these clusters gradually disperse due to gravitational interactions and stellar evolution, providing valuable insights into the dispersal and evolution of stellar systems within galaxies. Well-known open clusters include the Pleiades (M45) in the constellation Taurus and the Beehive Cluster (M44) in the constellation Cancer.



Figure 3.1: The open star cluster NGC 2547 (left) contains young, bright stars roughly 30 million years old that are loosely gravitationally bound and will spread apart over time. By contrast, the globular cluster 47 Tucanae (NGC 104) contains millions of stars about 13 billion years old that have been bound in the spherical cluster their entire lives.

3.2.1 NGC 6709:

NGC 6709 is an open cluster located in the constellation Aquila (the Eagle) which is some 5° to the southwest of the star Zeta Aquilae. It is situated toward the center of the galaxy and its distance from Earth is around 3,510 light-years. This cluster was discovered by astronomer William Herschel in 1784. It is designated as NGC (New General Catalogue) 6709 and is also known as Caldwell 55. The cluster is relatively young, estimated to be around 150 million years old, about the same as the Pleiades.

NGC 6709 is a relatively compact open cluster with a diameter of about 10-12 light-years. It contains a significant number of stars, estimated to be around 200 to 300 members. The cluster's central region appears denser and more concentrated than its outer part. The stars in NGC 6709 are predominantly main-sequence stars, which indicates their relatively young age. NGC 6709 likely contains stars of various masses, from low-mass stars to more massive ones. The core radius of NGC 6709 is 2.2 ly (0.68 pc) and the tidal radius 26.4 ly (8.08 pc). It contains two Be stars and one of them is a shell star. There is one candidate, a red giant member. Variable stars in NGC 6709 can be of different types, including pulsating variables, eclipsing binaries, or eruptive variables. The study of variable stars in the cluster can provide insights into stellar physics, stellar evolution, and other astrophysical processes.

NGC 6709 is an interesting target for astronomers studying star formation and the dynamics of open clusters. By examining the properties and distribution of stars within NGC

6709, researchers can gain insights into the cluster's formation history and its interaction with the surrounding interstellar medium.

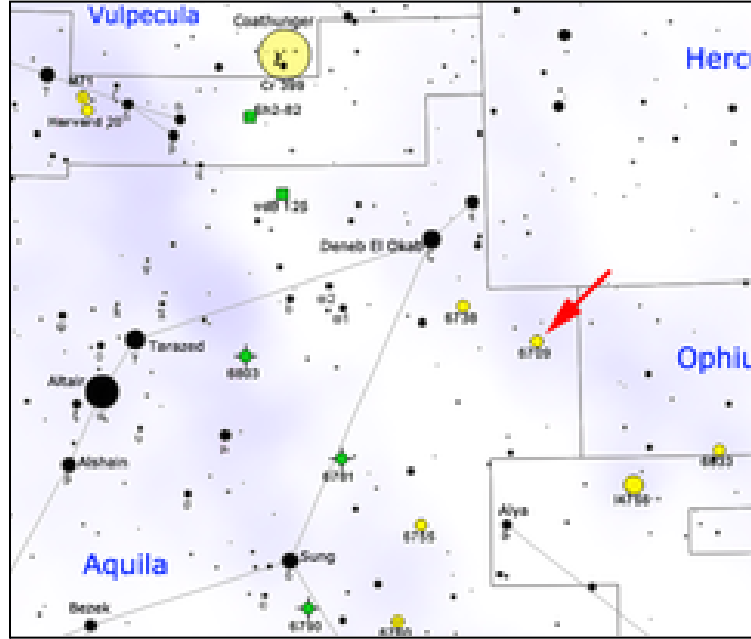


Figure 3.2: Position of NGC 6709: The red arrow indicates the position of NGC 6709 star cluster in the Aquila constellation.

4. Data Acquisition and processing:

The data used in this work was from the NGC 6709 star cluster captured by the Devasthal Fast Optical Telescope (DFOT). DFOT is a 1.3-meter aperture optical telescope, and is operated by Aryabhata Research Institute of Observational Sciences (ARIES), Nainital. The data consists of observations taken on 10 nights spanned over a period of 388 days or about an year (October 09, 2021 - October 31, 2022). Data from each night contains multiple frames of $2k \times 2k$ dimension. All the frames were captured in R band with an exposure time of 10 sec each and stored in fits file format.

The raw data was transformed using astrometry. This aligned the stars of all frames, such that each star was within 1 arcsec in another frame. Stars were detected from each frame of each night. The frame containing the maximum number of stars was used as a reference frame. This frame was used to match the RA and DEC of detected stars in other frames and used later to plot light curves.

Following log table contains the information about the data from each night.

Night	Date	No. of Science Frames used	Time and Duration of observation	
			JD	Hrs
1	09/10/2021	375	0.069104	1.658507
2	05/11/2021	160	0.030036	0.720864
3	06/11/2021	246	0.045887	1.101284
4	16/11/2021	178	0.032571	0.781703
5	17/11/2021	237	0.044203	1.060869
6	20/11/2021	205	0.037779	0.906703
7	19/03/2022	360	0.065592	1.574202
8	28/03/2022	280	0.071885	1.725247
9	10/04/2022	280	0.068416	1.641978
10	31/10/2022	180	0.032235	0.773647

Log table of data from 10 nights, providing information about science frames and duration of observations.

4.1 Cleaning:

Bias frames capture the inherent electronic noise present in the camera system. These frames are obtained by taking multiple exposures with zero integration time or extremely short exposure times, ensuring that no astronomical signal is recorded. By subtracting the bias frame from science or flat frames, unwanted noise like readout noise and dark current can be eliminated. For this, the bias frames are combined into a master bias frame to create a reference for calibration.

Flat frames are used to correct for non-uniformities in the optical system, such as dust particles, vignetting, and pixel-to-pixel sensitivity variations. Flat frames are obtained by taking exposures of a uniformly illuminated field, such as twilight sky or a diffusing screen. Multiple flat frames are combined using the median method to create a master flat frame. The master flat frame serves as a reference to normalize the science frames, compensating for pixel-to-pixel variations and ensuring accurate representation of the astronomical objects true intensities.

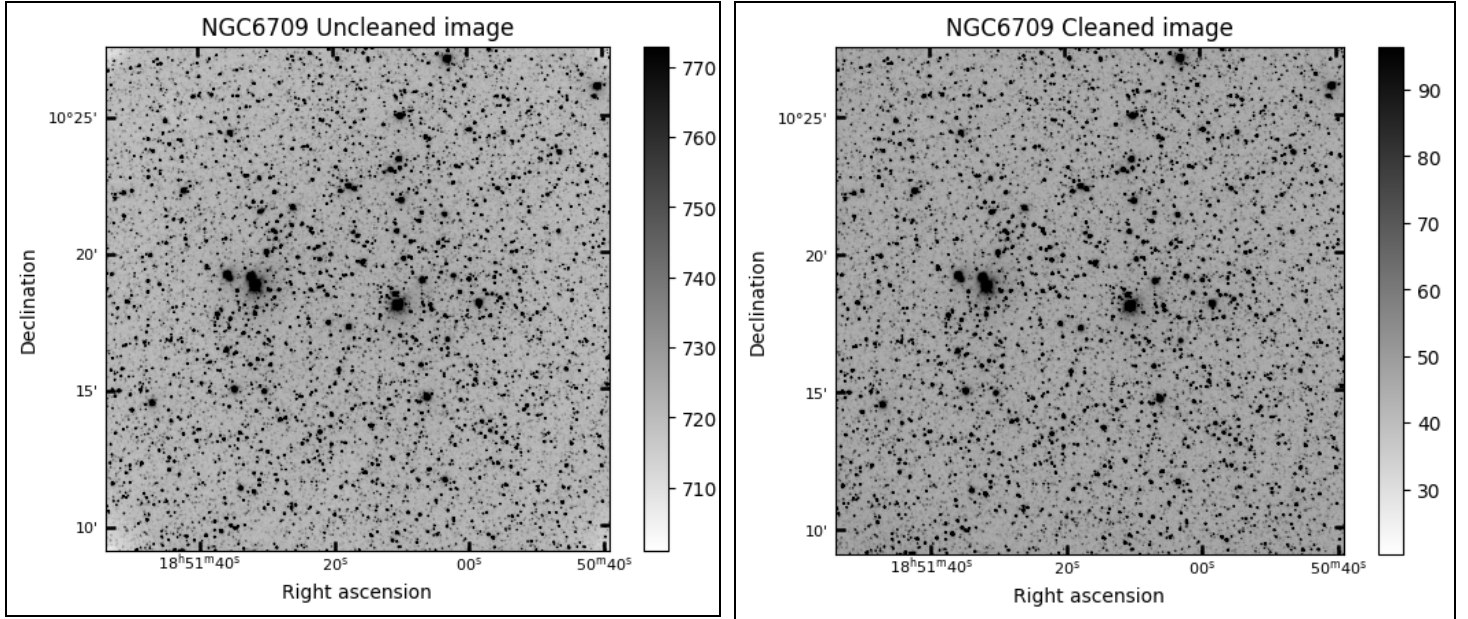


Figure 4.1: Uncleaned and cleaned images of NGC 6709 before and after running the cleaning process, respectively. The adjacent colorbar shows the pixel values.

Lastly, science frames are cleaned by subtracting the master bias frame and dividing by the master flat frame along with cosmic ray removal, using python snippets. For this purpose we used various functions from the astropy library. The image shows the cleaned and uncleaned image. It is clear that the pixel values have significantly dropped in the cleaned image, along with the correction in vignetting at the edges.

4.2 Aperture Photometry:

Aperture photometry is a technique used in astronomy to measure the total flux or brightness of a celestial object within a defined aperture or region of interest. It involves summing the pixel values within the aperture and subtracting the contribution from the background sky to obtain the net flux. Depending on the source, the aperture can be chosen to be circular, elliptical or rectangular.

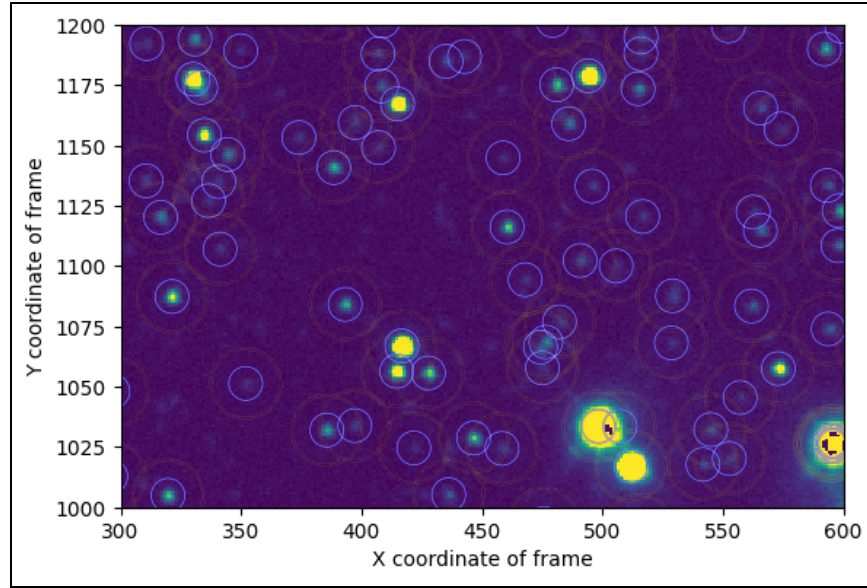


Figure 4.2: A region of NGC 6709 with aperture around the detected stars. The white circle is an aperture of radius 7 pixel and the region between two red circles is the annulus that accounts for the background of the aperture.

We have made use of the photutils library of python to perform the task of aperture photometry. We firstly used 5 apertures of radii 5,6,7,8 and 9 pixels. Corresponding to these radii, we got flux and using the formula below we calculated magnitude and its corresponding error:

$$\text{Magnitude} = -2.5 * \log_{10}(\text{Flux}) + C$$

Where, C is an optional constant for any additional corrections or offsets.

When performing aperture photometry, the choice of an optimum aperture size is important to ensure accurate and reliable flux measurements. The growth curve helps in determining this optimum aperture size. A growth curve represents the relationship between the aperture size used for measuring the flux of an astronomical object and the resulting flux or magnitude values obtained. It shows how the measured flux/magnitude changes as the aperture size increases.

After plotting the difference between largest aperture magnitude and other aperture magnitude against radii chosen, we got a growth curve for a particular star. Below is the plot for 5 and 15 numbers of stars.

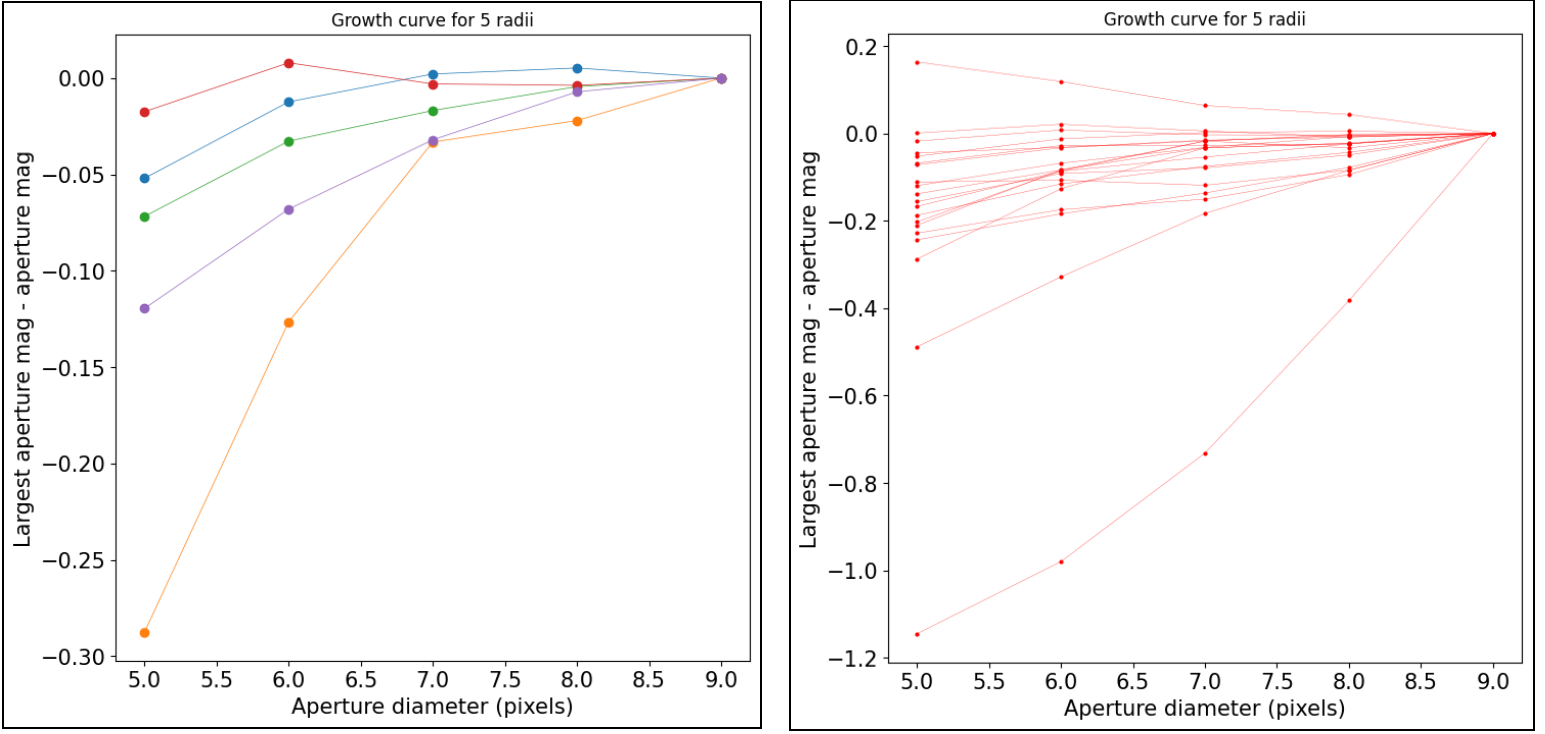


Figure 4.3: Growth curve for 5 stars(left) and 15 stars(right). Each circle represents a data point.

The optimum aperture size can be selected by considering the point on the growth curve where the flux values stabilize or show minimal change. This indicates the aperture size beyond which increasing the aperture does not significantly contribute to the flux measurement but may introduce more background noise or systematic errors. From above plots it is evident that, for most of the stars of this cluster, the curve becomes steady after radii of aperture size 7. Thus we used radii of 7 pixels as optimum aperture size.

4.3 Calibration:

After choosing optimum aperture size, the magnitude of all the detected stars in each frame was calculated using the above formula along with associated error. But the value was different from the standard value of magnitude. In order to resolve this issue, we calibrated the values of magnitude. Calibration involves obtaining a set of reference stars with known magnitudes in the same field of view. We made use of standard values of magnitude from Simbad.

SIMBAD (the Set of Identifications, Measurements and Bibliography for Astronomical Data) is an astronomical database of objects beyond the Solar System. As of 1 June 2020, SIMBAD contains information for 5,800,000 stars and about 5,500,000 non stellar objects (galaxies, planetary nebulae, clusters, novae and supernovae, etc.)

Calibrating for each night is important in photometric analysis for accurate measurements due to variations in atmospheric conditions, instrumental parameters, sky background, and

photometric zero point. It ensures consistency and reliable data across different observation sessions, especially for long-term monitoring. Hence different calibration values were used for each night. In order to get actual values of magnitude from SIMBAD we used data from RA and DEC from the first frame of each night.

Next we plotted the graph between values of magnitude obtained from SIMBAD against that obtained from our python code. Below is one such plot from the data of the first night.

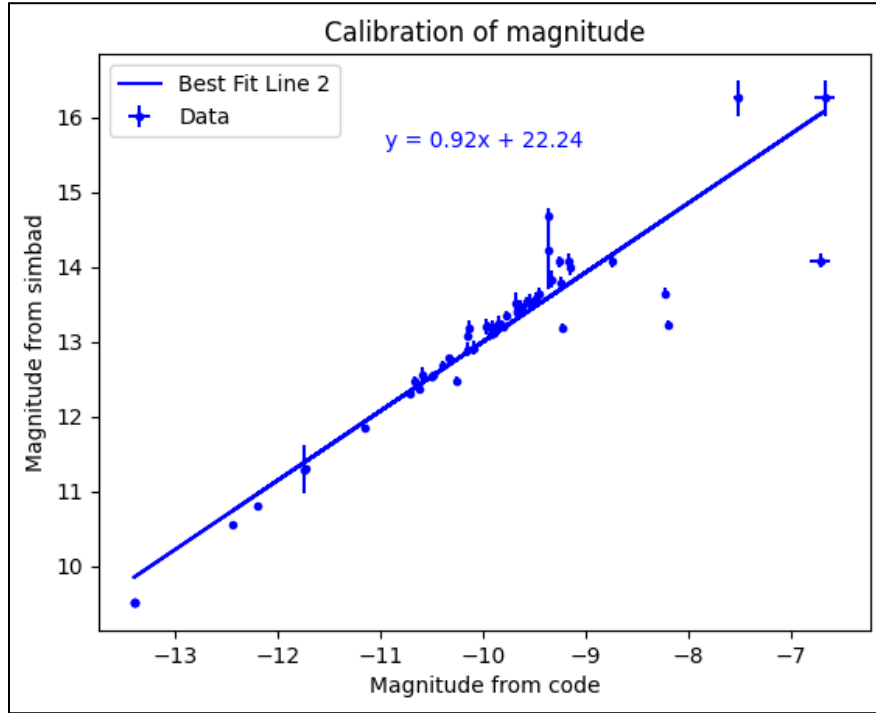


Figure 4.4: Best fit curve for magnitude values from SIMBAD against magnitude values from the code. An error bar for both the axes is also shown.

By measuring the fluxes of these detected stars and comparing them to their known magnitudes, a transformation equation can be derived. For this purpose, a best fit line was plotted and its equation was used as a transformation equation. This transformation equation was then applied to the measured magnitude of the stars in NGC 6709 to obtain their instrumental magnitudes.

Only for nights which have the percentage error in deviation from expected value of slope (i.e slope = 1) more than 10%, the correction in slope is taken into account. While for data from other nights, only correction in intercept is taken into consideration.

Night	Date	No. of stars in selected frame	No. of stars detected in SIMBAD (R band)	Intercept of best fit curve	Slope of best fit curve	Error in slope
1	09/10/2021	5507	59	22.24	0.92	8%
2	05/11/2021	4097	53	23.47	1.04	4%
3	06/11/2021	5141	55	22.55	0.95	5%
4	16/11/2021	3187	54	23.49	1.04	4%
5	17/11/2021	3160	57	23.04	1.01	1%
6	20/11/2021	2493	55	22.86	0.99	1%
7	19/03/2022	2963	53	21.35	0.86	14%
8	28/03/2022	4236	54	22.11	0.93	7%
9	10/04/2022	4156	56	20.92	0.84	16%
10	31/10/2022	2969	51	23.27	1.03	3%

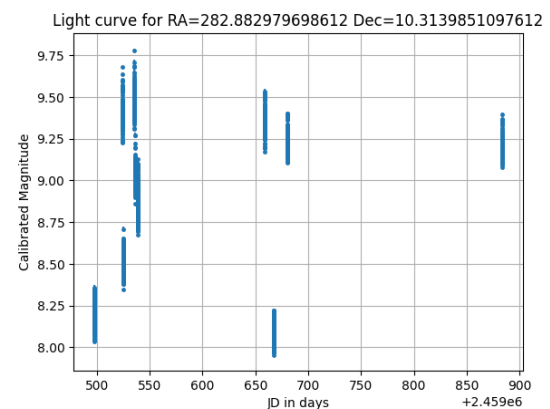
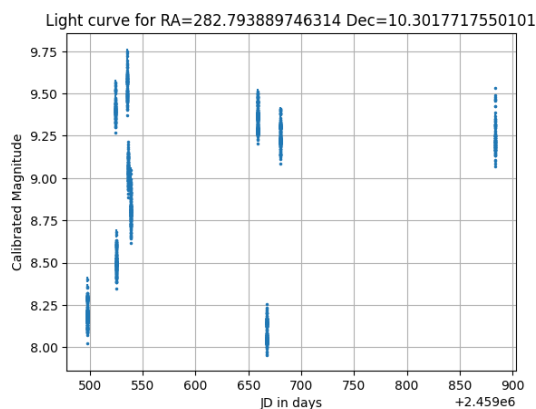
Log table of data after detection of stars in SIMBAD

The table shows the number of stars detected in SIMBAD each night. It also includes the corresponding value of calibration added to obtain the calibrated magnitude value for each star on a particular night.

4.4 Light Curves Analysis:

A light curve is a graph showing the changes in brightness of an object over time. It is crucial for studying variable stars, exoplanets, and transient events like supernovae. Light curves help identify variability, determine periods and changes in periods, probe exoplanets through transit observations, study stellar pulsations, and track transient phenomena. By analyzing the patterns in the light curve, astronomers gain insights into the nature, evolution, and physical properties of celestial objects.

Below are the light curves for some stars with RA DEC mentioned. Here the data from all the 10 nights is combined to get the light curve which is over a time period of 388 days.



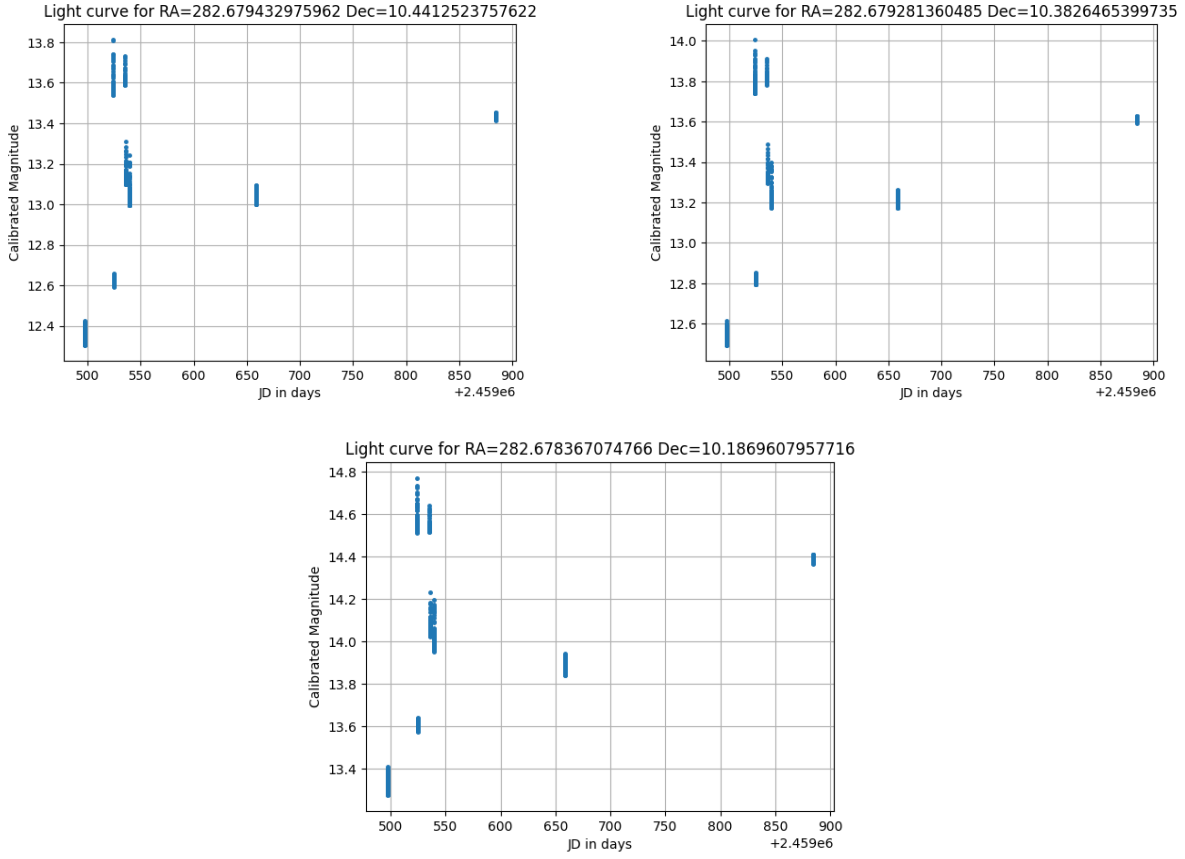


Figure 4.5: Light curves of 5 stars over a period of 388 days. RA and DEC values of these stars are mentioned on their respective plots.

4.5 Period and Phase estimation:

We have used the Lomb-Scargle algorithm to get the period of variability. This method is a widely used method in astrophysics for analyzing unevenly sampled time series data. It is particularly useful for detecting periodic signals in phenomena like variable stars and exoplanet transits. The algorithm involves preprocessing the data to remove biases, creating a frequency grid, calculating the power associated with each frequency, and estimating the significance of the detected signals. By comparing the power values to the expected distribution for white noise, significant periodicities are identified. The algorithm generates a periodogram, which visualizes the power values across frequencies. This allows astronomers to identify peaks and candidate periods in the data. The Lomb-Scargle algorithm is a powerful tool for uncovering hidden periodic signals in irregularly sampled data, contributing to our understanding of various astronomical phenomena and their underlying mechanisms.

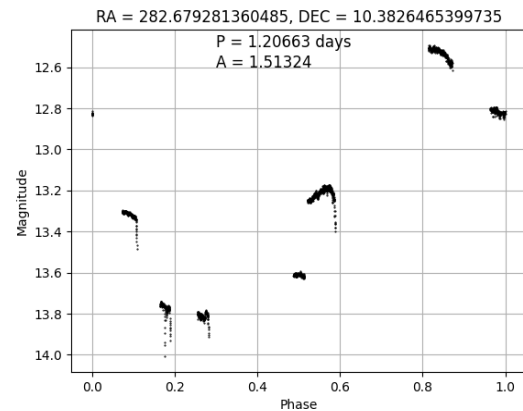
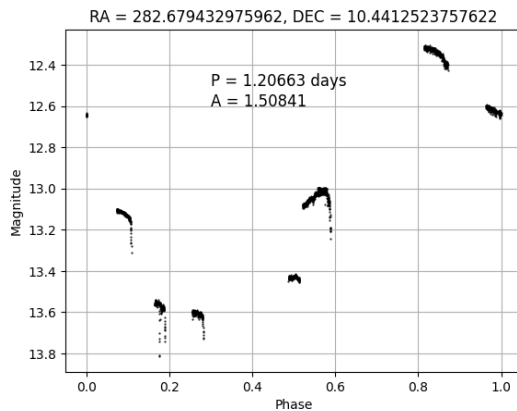
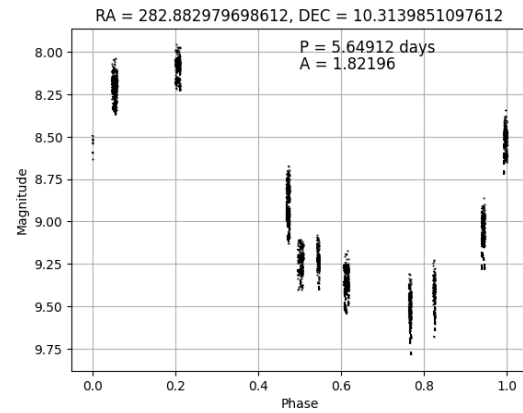
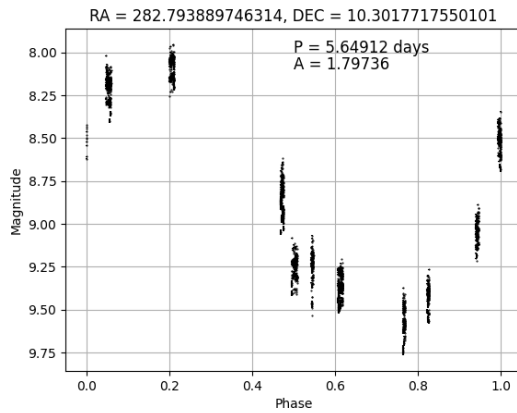
Next phase is also determined from the period obtained from Lomb-Scargle algorithm using formula:

$$phase = \frac{(time-t_0)}{period} - \int \left(\frac{(time-t_0)}{period} \right)$$

In this formula the *phase* represents the normalized phase of the signal at a specific time. Here, *time* is the specific time at which the phase is being calculated, *t₀* is the reference time or the starting point in the time series of data and *period* is the calculated period obtained from the Lomb-Scargle algorithm. Lastly, *int()* denotes the integer part of the division.

The amplitude of a variable star refers to the difference in brightness between its maximum and minimum values during a complete cycle. It is determined by analyzing a phase-magnitude curve, which plots the star's brightness against its phase. From the curve, the maximum and minimum magnitudes are identified, and the amplitude is calculated by subtracting the minimum magnitude from the maximum magnitude. The amplitude provides valuable information about the star's variability and can be used to classify different types of variable stars.

Plotting Magnitude against the phase calculated from the above formula, we get the following plots. These plots are for a particular star, whose RA DEC value is mentioned on the plot. Period and Amplitude are also determined for these stars.



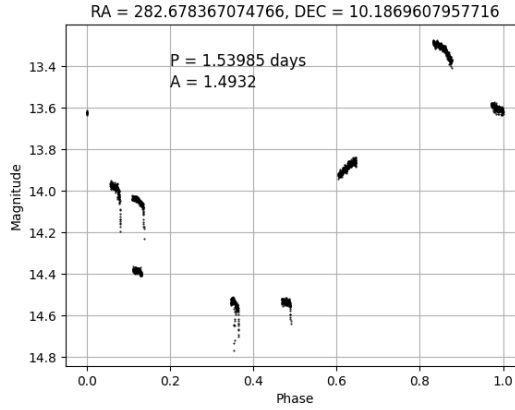


Figure 4.6: Phase - Magnitude curves for light curves of corresponding stars plotted previously.

5. Summary and conclusion:

After analyzing the above plots we were able to detect some variable stars from the NGC 6709 star cluster. Below table summarizes the results.

Star No.	RA	DEC	Mean Magnitude	Mean magnitude error	Period in days	Amplitude	Star identified in SIMBAD query
1	282.7938897	10.30177176	8.8664	0.002039	5.64912	1.79736	HD 229716 -- Spectroscopic Binary
2	282.8829797	10.31398511	8.86954	0.002073	5.64912	1.82196	BD+10 3697 -- Red Supergiant
3	282.6794330	10.44125238	12.99629	0.023878	1.20663	1.50841	HD 229684 -- Star
4	282.6792814	10.38264654	13.182879	0.028266	1.20663	1.51324	UCAC4 502-093343 -- Star
5	282.6783671	10.18696080	13.934683	0.056877	1.53985	1.4932	Gaia DR3 4311551504760695808 -- Star

Summary of detected variable stars in NGC 6709

The table shows the RA DEC values of detected variable stars. As we have calibrated the magnitude with the true magnitude of the star, the sky condition effects are taken into consideration.

This analysis was done over a data covering longer duration of time, but with low data points and their uneven distribution across the period of study. Out of 10 nights studied, 5 of them were of the same month. This might result in error while extrapolating light curves to get phase and magnitude from phase-magnitude diagrams. In order to overcome this issue, more data with a good number of frames per night needs to be studied to make concrete conclusions.

Also here, we have used aperture photometry as a method to detect stars and to calculate their magnitude. As this method captures flux within chosen aperture size, there might be cases where extra flux is taken into account due to adjacent stars present within the aperture. This is common with star clusters where many eclipsing binary or double star systems are often found. To resolve this problem, another method called PSF (Point Spread Function) photometry can be used. The method works by modeling the blurring effect called PSF, that occurs when light from a point source is spread out by the imaging system. The PSF is a mathematical representation of this blurring effect, taking into account factors like atmospheric turbulence and imperfections in the optics. By comparing the modeled PSF with the observed image, the photometry algorithm can estimate the flux or brightness of the source.

6. References:

- 1) Y.C. Joshi, Ancy A. John, J. Maurya, A. Panchal, Brijesh Kumar, Santosh Joshi.
'Variable stars in the field of intermediate-age open cluster NGC 559'.
- 2) YC Joshi, T Bangia, MK Jaiswar, J Pant, K Reddy, S Yadav
'ARIES 130-cm Devasthal Fast Optical Telescope—Operation and Outcome'
Journal of Astronomical Instrumentation 11 (04), 2240004
- 3) Simbad reference : <https://en.wikipedia.org/wiki/SIMBAD>
- 4) SIMBAD Query: <https://simbad.u-strasbg.fr/simbad/sim-fcoo>
- 5) Understanding variable stars by John R. Percy (Cambridge University Press, 2007).
- 6) Image references:
 - a) <https://slideplayer.com/slide/4073563/>
 - b) https://www.wikiwand.com/en/NGC_6709
 - c) <https://www.astronomy.com/science/what-is-the-difference-between-a-globular-star-cluster-and-an-open-star-cluster/>